Oculomotor abnormalities in children with Niemann-Pick Type C

Blundell, James; Frisson, Steven; Chakrapani, Anupam; Gissen, Paul; Hendriksz, Chris; Vijay, Suresh; Olson, Andrew

DOI:
10.1016/j.ymgme.2017.11.004

Document Version
Peer reviewed version

Citation for published version (Harvard):
Blundell, J, Frisson, S, Chakrapani, A, Gissen, P, Hendriksz, C, Vijay, S & Olson, A 2018, 'Oculomotor abnormalities in children with Niemann-Pick Type C', *Molecular Genetics and Metabolism*, vol. 123, no. 2, pp. 159-168. https://doi.org/10.1016/j.ymgme.2017.11.004

Oculomotor abnormalities in children with Niemann-Pick Type C

*James Blundell, PhD, Steven Frisson, PhD, Anupam Chakrapani, MD, Paul Gissen, MD,

Chris Hendriksz, MD, Suresh Vijay, MD, *Andrew Olson, PhD

James Blundell, The University of Birmingham, School of Psychology
Steven Frisson, The University of Birmingham, School of Psychology
Anupam Chakrapani, Great Ormond Street Hospital for Children
Paul Gissen, Great Ormond Street Hospital for Children and University College London Institute of Child Health
Chris Hendriksz, Salford Royal NHS Foundation Trust, University of Pretoria, Paediatrics and Child Health
Suresh Vijay, Birmingham Children's Hospital
Andrew Olson, University of Birmingham, School of Psychology

Corresponding Author:
James Blundell
School of Psychology
University of Birmingham
Birmingham, B15 2TT
Phone: +44 (0)121 414 4932
Fax: +44 (0)121 414 4897
j.m.blundell@bham.ac.uk

Keywords: Niemann-Pick C, supranuclear gaze palsy, eye-tracking, ocular motor**,** neurodegenerative disease, diagnosis

Acknowledgments

The authors wish to thank the patients and families who participated in the study. This study was supported by a CASE studentship funded jointly by the ESRC and The MPS Society and additional support was provided by Actelion Pharmaceuticals Ltd. and the Birmingham Children's Hospital Charity (BCHRF230).

Abstract

Niemann-Pick type C (NP-C) is a rare recessive disorder associated with progressive supranuclear gaze palsy. Degeneration occurs initially for vertical saccades and later for horizontal saccades. There are studies of oculomotor degeneration in adult NP-C patients [1, 2] but no comparable studies in children. We used high-resolution video-based eye tracking to record monocular vertical and horizontal eye movements in 2 *neurological* NP-C patients (children with clinically observable oculomotor abnormalities) and 3 *pre-neurological* NP-C patients (children without clinically observable oculomotor abnormalities). Saccade onset latency, saccade peak velocity and saccade curvature were compared to healthy controls (N=77). NP-C patients had selective impairments of vertical saccade peak velocity and vertical saccade curvature, with slower peak velocities and greater curvature. Changes were more pronounced in *neurological* than *pre-neurological* patients, showing that these measures are sensitive to disease progress, but abnormal curvature and slowed downward saccades were present in both groups, showing that eye-tracking can register disease-related changes before these are evident in a clinical exam. Both slowing, curvature and the detailed characteristics of the curvature we observed are predicted by the detailed characteristics of RIMLF population codes. Onset latencies were not different from healthy controls. High-resolution video-based eye tracking is a promising sensitive and objective method to measure NP-C disease severity and neurological onset. It may also help evaluate responses to therapeutic interventions.

Niemann-Pick Disease type C (NP-C, OMIM #257220) is a lysosomal storage disorder caused by abnormal intracellular lipid accumulation which results from a mutation in genes encoding either NP-C1 (95% of patients) or NP-C2 (5%) proteins [3, 4]. Clinical symptoms of NP-C are progressive and are primarily neurological. One of the earliest, and most distinct, neurological symptoms of NP-C is vertical supranuclear gaze palsy (VSGP) [5–7]. Initially only vertical eye-movements are affected, but later both horizontal and vertical movements become abnormal [8]. This results from cell loss in the rostral interstitial nucleus of the medial longitudinal fasciculus (RIMLF), responsible for vertical saccades, and eventually in the paramedian pontine reticular formation (PPRF), responsible for horizontal saccades. The integrity of excitatory burst neurons in these nuclei is related to peak saccade velocity, which has been shown to be a useful index of dysfunction in the RIMLF and PPRF [9, 10]. In addition, a strictly upward movement requires balanced excitation in two populations of neurons. Neurons in RIMLF that code upward and left torsion must be balanced by neurons that code upward and right torsion so that the two torsional instructions cancel out [10]. Damage that is distributed over RIMLF will often produce asymmetries in the two populations coding for vertical movements. We will show that the details of RIMLF population coding, as described by Crawford and Vilis [11] in their stimulation and activation study, predict both the slowing and curvature that we see in our NP-C results. Our results, as a consequence, add evidence to support the functional description they provide.

Detailed reports of oculomotor dysfunction exist in adult NP-C patients [2, 8], where vertical saccade degeneration is absolute. Detailed information about the onset and progression of vertical saccade degeneration during early stages of the disease, most often in childhood, is lacking. This is a clinically important gap because the only approved treatment of NP-C (miglustat, or Zavesca, Actelion, a small iminosugar that inhibits glucosylceramide synthesis) slows neurodegeneration [12–15] but is prescribed only once neurological involvement (e.g. gaze palsy or ataxia) has been detected. Established clinical severity scales aimed at tracking the neurological progression of NP-C exist [16]. However, these are based

on a bedside examination of eye movements. Bedside examination will not be able to measure changes with the same sensitivity as modern eye-trackers which sample eye position up to 1000 times a second. These offer the potential to detect the eye movement changes much earlier. We tested techniques designed to identify changes to eye movements, and, therefore, the onset of neurodegeneration earlier. This could allow clinicians to make decisions sooner that are aimed at maintaining patient abilities at the highest possible level. In this study, we established norms for oculomotor developmental change in a large sample of control children and compared NP-C patients to the control range to see if this allowed neurological impairment to be detected using eye-tracking before it is evident with standard clinical methods.

Methods

Patient Information. Five paediatric NP-C patients were recruited from NP-C clinics at Birmingham Children's Hospital and Great Ormond Street Hospital (mean age= 6.3, range=2–9years, M/F=3/5). Inclusion criteria included a diagnosis confirmed by cultured fibroblasts cholesterol esterification rate analysis and filipin staining of unesterified cholesterol. In addition, patients must have been aged above 2-years and be neurologically capable of attending to the oculomotor assessment. There were no other exclusion criteria (e.g. none related to oculomotor control). Clinical scores were obtained for patients using Yanjapnin NP-C Clinical Severity Scale [7]. Demographics and overall clinical scores are shown in Table 1 (detailed clinical scores in Appendix A). Three patients were neurologically asymptomatic and, in particular, did not have oculomotor abnormalities in clinical testing (*pre-neurological NP-C,* disability score=0). The two neurological patients (NP-C03 and NP-C05) had clinically observable mild/functional VSGP (i.e. vertically eye movements were not completely abolished, but initiation depended on the use of a proceeding head-thrusting and/or blinking). No patients were receiving medication for seizures (e.g. benzodiazepines) that could disrupt eye movements. Patients were compared to data from 77 healthy controls

with no history of major medical, neurological or psychiatric illness (mean age=11.86, range=2–20 years, M/F=43/34).

Table 1 about here

Procedure. The study was approved by the local research ethics committee (South Birmingham LREC) and patient parents/guardians provided written informed consent. Participants were tested in a dimly lit environment, 60 cm away from a 32 × 26 cm CRT-monitor (resolution=1024 by 768; refresh rate=60 Hz). Monocular eye movements were recorded at 1000 Hz (video-based EyeLink® 1000, tower mount; SR Research Ltd.). Eye movements were calibrated to an accuracy of at least 1° of visual angle. A chin rest was used to stabilize each participant's head in relationship to the camera monitoring the position of the pupil and corneal reflection.

The oculomotor task consisted of 48 trials. Trials began with the target, an elephant face (size=1.5°), presented centrally for 1000 milliseconds (ms). The target disappeared and reappeared at one of four surrounding locations (above, below, left and right; eccentricity=10°) for 1000ms. Participants were instructed to fixate the elephant and follow it quickly and accurately when it moved. For younger participants (2-5 years), interstimulus intervals included a salient animated cartoon flower that rotated at the centre of the screen to increase task engagement and reduce inattention.

Statistical Analysis. Raw data were plotted to identify saccades visually. The first eye movement toward the target was marked, along with the 1000 samples that immediately preceded and followed the movement. These 1000 samples, where the eye was relatively stable, were used to calculate a velocity threshold (velocity mean ± 3SD) that allowed the

saccade to be systematically identified. Trials where blinks disrupted saccadic movements were eliminated.

Development of saccade onset latency, saccade peak velocity and saccade curvature in healthy controls was characterised using developmental trajectories [17]. For each measure, three functions (a constant value, or *intercept only,* linear and quadratic functions) were fit to control data and the best was selected using Akaike Information Criterion values (AIC) and Akaike weights [18]. AIC-based model selection is preferable to model selection using p-values because it emphasizes the weight of evidence for models in a candidate set. One model or several models can receive support and there is an explicit trade-off between fit and number of model parameters to guard against overfitting [18][9]. This method distinguishes cases where several models provide relatively good accounts of the data (relatively equal probabilities split across several models) from cases where one model is clearly better than the others (one model has high probability, all others low).

We used linear mixed effects models (LME) for statistical analysis of developmental trajectories and group differences [19]. Random and fixed effects were selected using AIC following the method described by Diggle [20]. We report group analyses for *pre-neurological* patients, where we want to know if eye-tracking can reveal group differences that are not clinically apparent (and don't depend on the most severe patients). We expect to see differences between *neurological* patients and controls, and, in fact, these are usually apparent at the level of individual patients. We report individual results for all patients. In the group analysis, there were fixed effects for *Group* (to test for differences between patients and controls), *Age* (to test for differences in developmental trajectories) and *Condition* (to test whether abnormalities were confined to particular stimulus locations). Main effects of *Group* are found if performance is worse in the patient group across all ages. Interactions with *Age* occur if development is slower in the patient group, if it is slower at a particular stimulus location

(Age X Group or Age X Condition interactions) or if the developmental trajectory is slower for patients in only some conditions (Age X Condition X Group interaction).

To examine performance in individual patients, we, first, calculated ninety-five percent prediction intervals for developmental trajectories in controls by fitting intercept-only, linear and quadratic functions to upper or lower 95% t-value cutoffs. We used AIC to choose the function that best described the trajectory of the upper or lower limit. Individual NP-C patients who were outside the prediction interval were reliably different from controls. Individual patients were compared to controls using the equivalent of z-scores, calculated from the upper or lower endpoints of the prediction intervals, rather than from noisier age-specific samples. Our method smooths the prediction intervals, borrowing information from adjacent regions on the developmental curve, in the same way the function describing the mean is smoothed. We label these z_{pi}.[1]

Results

Saccade Onset Latency. Saccade onset latency in normally developing control children was described best by a quadratic function (quadratic ΔAIC/AIC*w* 0/.99; linear ΔAIC/AIC*w* = 13.04/.01; intercept ΔAIC/AIC*w* = 26.48/.01). Developmental change occurred between 2 and 10 years with little improvement after 10 (Figure 1). The rate of development differed across target locations. LME analysis (random intercept for participants), revealed an interaction between target location and age (*Condition X Age*^{2} model ΔAIC/AIC*w* = 0/.99; *Condition + Age* ^{2} model = 13.83/.00; detailed model results in Appendix B). To see if trajectories were systematically grouped, a model distinguishing horizontal from vertical trajectories was compared to a model with trajectories for each target location. Both models

[1] Specifically, for values above the mean, $SD_{pi} = (PI_{upper} - mean)/1.96$ and $z_{pi} = Y_{patient}/SD_{pi}$, where PI_{upper}= upper boundary of the 95% prediction interval; *mean* = the mean predicted by the fit to control values; and $Y_{patient}$ = patient's observed data value. Values below the mean were calculated in the same way except the 95% prediction interval boundary (PI_{lower}) used the lower boundary since boundaries were not necessarily symmetric.

provided equivalent descriptions of healthy development (ΔAIC < 1), so the simpler horizontal/vertical model was preferred. Onsets were initially slower but development was steeper for vertical target positions (Figure 1).

Figure 1 about here

Evidence of a difference between *pre-neurological NP-C* patients and controls was weak. The model with strongest support did not distinguish patient and control groups (*Condition X Age*^{2} model ΔAIC/AIC*w* = 0/.52; strongest model with group effect: *Condition X Age*^{2} + *Group* model = 1.38/.26; model results are listed in Appendix C), and mean *pre-neurological* patient onset times were normal (mean z_{pi} horizontal = 0.53 / vertical = - 0.17).

Results for individual patients did not highlight significant exceptions to this pattern. Only the onset time of the youngest *pre-neurological* patient (2 years) was longer than expected (z_{pi} = -2.17) and for left targets only. Deficits or borderline deficits were more apparent in the vertical movements of *neurological* patients. They were slower to initiate saccades (NPC-03, z_{pi} = -2.17; NPC-05, z_{pi} = -2.16).

Saccade Peak Velocity. Peak velocity, on average, slowed somewhat with age, and the amount of change depended on the quadrant. The best model was linear (*Condition X Age* model ΔAIC/AIC*w* = 0/.86; *Condition* + *Age* model ΔAIC/AIC*w* = 3.6/.14). Previous studies reporting velocity changes with age have differed [see review in 21], but slowing in the early years is one of the reported patterns [e.g. 22], so this is not an isolated result.

Eye movement peak velocities depend on how far the eyes move. Velocities are systematically higher for longer saccades. This raises the question of whether developmental differences in peak velocity were driven by differences in saccade amplitude. To factor out the influence of amplitude, which will also be important when we turn to patient data, we

predicted peak velocity using amplitude and then modelled the component of velocity left over after amplitude was factored out (velocity residuals).

There was still an interaction between age and condition (*Condition X Age* model ΔAIC/AIC*w* = 0/.98; *Condition + Age* model ΔAIC/AIC*w* = 8.6/.01). Velocity decreased with age, but only for downward saccades (*Age* model ΔAIC/AIC*w* = 0/.99; intercept only model ΔAIC/AIC*w* = 10.6/.005; Figure 2A). Other directions did not change (left: intercept only model ΔAIC/AIC*w* = 0/.66; *Age* model ΔAIC/AIC*w* = 1.3/.34; right: intercept only model ΔAIC/AIC*w* = 0/.67; *Age* model ΔAIC/AIC*w* = 1.4/0.33; top: intercept only model ΔAIC/AIC*w* = 0/.72; *Age* model ΔAIC/AIC*w* =1.9/.28).

Amplitude was also an issue when quantifying group differences in peak velocity. Patients could have lower peak velocities either from slowing or simply because saccades often fell short of their targets. Plotting saccade amplitude and velocity together in Figure 2B shows that changes in velocity were not generally a simple consequence of making shorter saccades. Confidence intervals describing the control range of amplitudes and peak velocities (error bars) show that, for bottom targets, 3 patients were slower than controls, but only one had abnormally shortened saccades. For top targets, two patients were slow, but only one made shorter saccades. Our group analyses factor out these amplitude differences, by using velocity residuals, to quantify the component of velocity that is independent of the length of the saccade.

After factoring out amplitude differences, *pre-neurological* patients were slower than controls, but not in all positions, resulting a *Group X Condition* interaction (all of the top 3 models, which only differed by a maximum ΔAIC of 1.23, included a *Group* X *Condition* interaction). The first model without the interaction was clearly worse (*Condition* X *Age* + *Group* X *Age* ΔAIC/AIC*w*=3.8/.06). *Pre-neurological* patients were slower than healthy controls for bottom targets only (*Age* + *Group* ΔAIC/AIC*w*=0/.99; *Age* only

ΔAIC/AIC*w*=10.4/.006). There were no differences at other target locations (intercept-only model always better).

In individual results, deficits were more pronounced in *neurological* compared to *pre-neurological* patients. Peak velocity of downward saccades was clearly slower in both of the *neurological* patients (filled symbols; NPC-03, z_{pi}=-3.10; NPC-05, z_{pi} = -4.11). It was also slower in the eldest *pre-neurological* patient (NPC-04, z_{pi} = -2.37; *pre-neurological* patients are open symbols). In the other directions, peak velocities of both *pre-neurological* and *neurological* patients were mostly within the range of controls, although there was some evidence of slowing in horizontal movements for the two neurological patients (NPC-03, right z_{pi}= -2.31; NPC-05, left z_{pi}=-1.53).

Figure 2 about here

Saccade Curvature. Raw eye movement data revealed marked curvature in patient saccades. Figure 3 illustrates how curved vertical saccades had become. Horizontal saccades were unaffected when compared to age-matched controls.

Figure 3 about here

To quantify curvature and compare patients to healthy controls we measured eye position on the dimension orthogonal to the saccade (e.g. horizontal for vertical saccades). The standard deviation of this value summarised the degree of curvature.

In healthy controls, development with age was best captured by a linear function (Linear ΔAIC/AIC*w*=0/0.91; Quadratic = 4.8/0.09; Intercept only = 67.6/0.00; Figure 4). There was an interaction between age and target location (*Condition X Age* model ΔAIC/AIC*w* = 0/.92; *Condition + Age* model = 4.85/.08; *Condition* model = 20.1/0.00). To see if trajectories were systematically grouped, a model coding each direction separately was compared to a model that only distinguished horizontal and vertical movements. The *Separate* model provided the best description (*Separate* model = 0.00 / 1; *Horizontal/vertical* model ΔAIC / AIC*w* = 55.4 / 0). Downward movements showed most developmental change, followed by left, upward and then right (which had very little change with age). Downward movements also showed the largest absolute levels of curvature, followed by upward movements. Left and right movements were least curved and nearly equal. It is worth noting that the differences in controls are small, even if they are statistically reliable.

Figure 4 about here

Comparing *pre-neurological* patients and healthy controls showed differences at particular locations (*Condition X Age X Group* model = ΔAIC/AIC*w* = 0/0.48, *Condition X Age + Condition X Group* model = 1.68/0.21, *Condition X Age + Condition X Group + Age X Group* model = 1.73/0.20). Group differences were most pronounced for bottom targets (ΔAIC/AIC*w*: *Age X Group* model = 0/0.83; *Age* model = 3.4/0.15), but top targets were different as well (ΔAIC/AIC*w*: *Age X Group* model = 0/0.55; *Age* model = 1.3/0.28). There was no effect of group for left or right targets ((ΔAIC/AIC*w*: left: *Age* model = 0/0.74; *Age X*

Group model = 2.1/0.26; right: *Intercept only* model = 0/0.52; *Group* model = 1.5/0.25). The scale of the change in curvature in vertical movements is evident in Figure 3.

Individually, both *neurological* patients and 2 of 3 *pre-neurological* patients were outside the normal range of curvature for vertical saccades (Figure 4, bottom). Both *neurological* patients had substantially curved downward saccades (NPC-03, z_{pi} = -26.74; NPC-05, z_{pi} = -5.65), but also clear upward changes (NPC-03, z_{pi} = -16.37; NPC-05, z_{pi} = -2.60). Two *pre-neurological* patients also exhibited clear changes in upward and/or downward movements (NPC-02, upward, z_{pi} = -3.19; NPC-04, upward, z_{pi} = -3.26, downward = -2.28). The unaffected patient was the youngest of the *pre-neurological* group (NPC-01, z_{pi} = -0.19).

Table 2 summarises results from all measures in all directions. Horizontal movements are almost entirely unaffected by the disease. Vertical movements are often affected. Curvature is affected first, with changes apparent even in pre-neurological patients and peak velocity is also often affected. Saccade onset can be affected, but usually only when the disease is more advanced.

Discussion

We have presented a high resolution assessment of oculomotor function from a cohort of paediatric *neurological* and *pre-neurological* NP-C patients (i.e. with and without clinically apparent oculomotor impairments). In both groups of patients there were impairments in saccade velocity and saccade curvature. Vertical saccades were more affected than horizontal saccades as would be expected with greater cell loss in the brainstem nucleus RIMLF compared to the PPRF [12].

Since excitatory burst neurons in the RIMLF are associated with peak saccade velocity and that RIMLF is known to be affected by the disease, velocity is a natural place to look for early signs of NP-C damage [12]. Velocity changes were, indeed, found in all of the

neurological patients, as expected, and in one of the three pre-neurological patients. This is exactly the pattern that is desirable for a good indicator. Changes were apparent in eye-tracking records before they were noticeable in the clinic, and they followed the pattern you would expect from a value that anticipates more serious changes to oculomotor control (i.e. the changes were apparent in the older patients, where the disease is likely to be more advanced, but less strong in younger patients) The lag with which subtle changes to peak velocity anticipate more substantial changes and the consistency of this lag across individuals is an important topic for future research.

A new result was that saccade curvature was an equally early or even earlier index of changes. Curved eye-movements to *oblique* targets have been reported previously in NP-C [23], but, given the way the eye-movement system is organised, curved saccades to oblique targets are expected when vertical movements are slowed. Oblique saccades become curved because the eye arrives at the horizontal target position earlier than the vertical position and the trajectory curves upward as the vertical component finishes late. In other words, curvature in oblique saccades is a simple consequence of velocity changes. Curved oblique saccades do not, however, predict that purely *vertical* saccades will also be curved. These should just be slower. We found that purely vertical saccades were curved, which cannot be explained by simple velocity changes.

Curved vertical saccades have been noticed before. Quinn [14] and Jitkritsadakul, Tansuhaj & Bhidayasiri [15] reported that early stage progressive supranuclear palsy (PSP) patients had curved saccades in the purely vertical direction. Leigh [16] speculated that this is an adaptive strategy whereby the patient starts to make a saccade with a horizontal component to increase the time available to generate the vertical component. Indeed, a recent case report describes an adult with NP-C who had severely affected downward saccades and upward saccades accompanied by a horizontal movement, which the authors interpreted as a strategic adjustment [24]. While an element of strategy cannot be ruled out in our patients, curvature was evident *before* vertical saccades were noticeably slower and the degree of

curvature was relatively small, compared to what would be detectable without an eye-tracker, so a strategic approach seems unlikely. The neural organisation of RIMLF, however, offers a better explanation.

Curved saccades are predicted from the way the RIMLF nucleus is organised to code vertical movements. Neurons in the RIMLF do not code up- or downward movements in isolation. Instead each neuron codes both a direction (up/down) and a rotation around the axis that runs from the pupil down the line of sight (torsion) [11]. This is because vertical movements involve the oblique muscles, which are the main muscles responsible for torsional movements, in addition to the inferior and superior rectus muscles that move the eye directly up and down.

Crucially, Crawford and Vilis [11], in their detailed study of RIMLF function, show that the neuronal populations dedicated to vertical movements do not code simple straight up and straight down directions. They code an oblique up or oblique down direction in addition to torsion (see their Figures 7 and 16). Normally, when RIMLF is coding straight vertical movements, the left and right oblique deflections cancel each other, in the same way that the torsional movements cancel, and movement is straight up or straight down. When one side of the RIMLF is inactivated, however, Crawford and Vilis noted that eye-movements had a left or right deflection in addition to slowing in the vertical direction. This means the coding system predicts exactly what we found in patients. When populations of neurons that must normally counterbalance are affected by disease, the eyes will be driven obliquely toward the side pointed to by the stronger population.

This explains the initial deflection, but not the return to the target. For the eyes to curve back toward the target position, eye-movements must be under the feedback control of an unaffected centre above the level of the RIMLF. In other words, there must be a level where the target is coded in the correct position that will force a correction. This also fits, however, current standard assumptions about eye-movement control [10, 25]. The exact details of how and where feedback control is implemented are still under investigation, but

there is agreement that a copy of the signal from RIMLF (a corollary discharge, which will contain the oblique error) is compared to the intended eye-position (under control of the superior colliculus) and the eye position is modulated until the error is eliminated [10, 25].

Two additional predictions follow from these accounts. The first is that curvature will be systematically to one side for up or down saccades and the second is that curvature will begin at the start of the saccade. Neither of these would follow from a source of measurement noise or an artefact that affects vertical measurements. It is clear from Figure 3 that both of these predictions were substantially upheld (only NP-C 03's upward saccades showed curvature on both sides of the vertical, and this is one of the most severe patients). In fact, movements up and down are not only consistently to one side, they tend to be curved to opposite sides for up and down movements. This is what Crawford and Vilis found when they inactivated one side of the RIMLF at a time. Horizontal deflections were to opposite sides for up and down saccades.

We assume, in the absence of other information, that NP-C will randomly affect populations of neurons in the RIMLF. Random damage is not guaranteed to affect one side of the nucleus more strongly, but that will often be the case. Following the logic of random damage affecting a bilaterally arranged structure, it should be possible for damage to be relatively equally spread across right and left RIMLF. This means that slowed saccades without curvature are possible, but should occur relatively rarely. In addition, as damage progresses, curvature could become either more or less pronounced. It is not guaranteed that the asymmetry will always get worse with time. As damage becomes more complete, in fact, there may be a tendency for slow or hypometric saccades to dominate, with curvature a less prominent feature.

As damage to RIMLF progresses, the total number of burst neurons firing in *any* part of the RIMLF will get noticeably smaller. Velocity and, eventually, saccade onset itself should be affected. This was the pattern we observed (see Table 2). The early appearance of curved saccades and velocity changes raises the possibility that video-based oculomotor

measurement could improve the sensitivity with which disease progression is tracked in NP-C [see also 9].

Our results show that high-resolution eye tracking has the potential to: 1) Provide sensitive metrics that track the course of neurodegeneration in paediatric NP-C patients, and 2) Identify the onset of neurological decline earlier than is currently possible with standard clinical approaches. This is particularly important for NP-C management since treatment, which slows neurological decline, is currently available only when there are measurable neurological effects. Our methods could detect onset of neurological decline earlier, so that patients are stabilized at a higher level of cognitive function. Sophisticated eye-tracking techniques, which have been the domain of specialised laboratories in the past, could move into clinical settings and contribute to sensitive assessments.

NP-C is a rare paediatric neurodegenerative disorder. Inevitably, this means there is some uncertainty about how well our results will generalise to a larger population of patients and about how well cross-sectional data reflects what happens, over time, in individuals. Note, however, that our method for comparing individual patients to the control population is what is needed for clinical decision-making. This measures when performance *in an individual* is exiting the range defined by a large population of normally developing control children. The control sample is large enough that our confidence in the normal range of control values can be relatively high. It is true that our group comparisons are based on small samples of patients, but there are already reliable differences in velocity and curvature based on the five patients that we report and the results are theoretically consistent with what is known about how RIMLF functions. Additional participants are unlikely to change the qualitative pattern that is emerging here, where abnormalities in eye-movements occur, although the exact scale and time course and the variability of changes will need to be followed in a larger sample. Longitudinal follow-ups could help us to understand the natural time course and degree of individual variability in the disease. Longitudinal data may also allow us to detect neurological involvement even earlier than we have been able to do here.

This is because an individual's *trajectory* of change could be noticeably abnormal before the absolute level of performance, at any single point, has exited the control range.

Conclusion. High-resolution video-based eye-tracking, using simple fixation tasks, can identify oculomotor changes in NP-C children earlier than is possible with clinical oculomotor assessments. A promising new metric, saccade curvature, measured impairments in patients both with and without diagnosed neurological involvement and peak velocity was also low in some pre-neurological patients. Longitudinal studies should be used to confirm our measures as a good marker of neurological onset and explore using them to monitor treatment effects in children with NP-C. Eye-tracking is high precision, but the tasks are relatively simple, quick and easy for children to do. Comparison with robust control data can highlight individuals who fall outside the normal range, and the approach we have outlined here is ideal for both clinical decision-making and working with data from rare diseases. Future studies could investigate the utility of eye tracking data to screen for NP-C in populations of patients that present with symptoms that are associated NP-C, for example, in patients with early-onset ataxia and / or frontotemporal dementia. It is thought that NP-C may be undiagnosed in some patient groups that display symptoms associated with NP-C, but where the symptoms are not diagnostic on their own [26–28] . Eye-tracking measures could contribute to identify those patients that warrant further follow-up investigation.

Ethics statement: All participants gave informed consent.

Author Disclosures:

This study was sponsored by University of Birmingham, UK. Dr. Blundell has received honoraria and travelling expenses from Actelion Pharmaceuticals to attend meetings. Received funding support from Actelion Pharmaceuticals and an ESRC Case studentship. Dr. Olson has received travelling expenses to attend meetings by Actelion Pharmaceuticals. Dr. Chakrapani has received honoraria, travelling expenses and travel funding support from Actelion, Shire, Lysogene, Biomarin and Nutricia. Prof. Gissen has received honoraria, travelling expenses and research funding support from Actelion Pharmaceuticals. Paul is a Senior Wellcome Trust Senior Clinical Fellow. Dr. Vijay has received sponsorship from Actelion Pharmaceuticals Ltd towards attendance at academic meetings. Prof. Hendriksz has no disclosures related to this manuscript, but general disclosures are Director of FYMCA Medical Ltd, Consultant for Actelion, Amicus, Biomarin, Inventiva Sanofi-Genzyme, Shire.

References

1. Abel LA, Walterfang M, Fietz M, et al (2009) Saccades in adult Niemann-Pick disease type C reflect frontal, brainstem, and biochemical deficits. Neurology 72:1083–1086 . doi: 10.1212/01.wnl.0000345040.01917.9d

2. Walterfang M, Abel LA, Desmond P, et al (2013) Cerebellar volume correlates with saccadic gain and ataxia in adult Niemann-Pick type C. Mol Genet Metab 108:85–9 . doi: 10.1016/j.ymgme.2012.11.009

3. Burlina A (2014) Niemann-Pick disease type C: Introduction and main clinical features. J Neurol 261:S525–S527 . doi: 10.1007/s00415-014-7382-z

4. McKay Bounford K, Gissen P (2014) Genetic and laboratory diagnostic approach in Niemann Pick disease type C. J Neurol 261:569–575 . doi: 10.1007/s00415-014-7386-8

5. Strupp M, Kremmyda O, Adamczyk C, et al (2014) Central ocular motor disorders, including gaze palsy and nystagmus. J Neurol 261:S542–S558 . doi: 10.1007/s00415-014-7385-9

6. Sevin M, Lesca G, Baumann N, et al (2007) The adult form of Niemann-Pick disease type C. Brain 130:120–133 . doi: 10.1093/brain/awl260

7. Salsano E, Umeh C, Rufa A, et al (2012) Vertical supranuclear gaze palsy in Niemann-Pick type C disease. Neurol Sci 33:1225–1232 . doi: 10.1007/s10072-012-1155-1

8. Abel LA, Bowman EA, Velakoulis D, et al (2012) Saccadic Eye Movement Characteristics in Adult Niemann-Pick Type C Disease: Relationships with Disease Severity and Brain Structural Measures. PLoS ONE 7:1–7 . doi: 10.1371/journal.pone.0050947

9. Ramat S, Leigh RJ, Zee DS, Optican LM (2007) What clinical disorders tell us about the neural control of saccadic eye movements. Brain 130:10–35 . doi: 10.1093/brain/awl309

10. Sparks DL (2002) The brainstem control of saccadic eye movements. Nat Rev Neurosci 3:952–64 . doi: 10.1038/nrn986

11. Crawford JD, Vilis T (1992) Symmetry of oculomotor nurst neuron coordinates about Listing's plane. J Neurophysiol 68:432–448

12. Patterson MC, Vecchio D, Jacklin E, et al (2010) Long-term miglustat therapy in children with Niemann-Pick disease type C. J Child Neurol 25:300–5 . doi: 10.1177/0883073809344222

13. Patterson MC, Vecchio D, Prady H, et al (2007) Miglustat for treatment of Niemann-Pick C disease: a randomised controlled study. Lancet Neurol 6:765–72 . doi: 10.1016/S1474-4422(07)70194-1

14. Sedel F, Chabrol B, Audoin B, et al (2016) Normalisation of brain spectroscopy findings in Niemann-Pick disease type C patients treated with miglustat. J Neurol 263:927–936 . doi: 10.1007/s00415-016-8051-1

15. Patterson MC, Mengel E, Vanier MT, et al (2015) Stable or improved neurological manifestations during miglustat therapy in patients from the international disease

registry for Niemann-Pick disease type C: An observational cohort study. Orphanet J Rare Dis 10:65 . doi: 10.1186/s13023-015-0284-z

16. Yanjanin NM, Vélez JI, Sc M, et al (2011) Linear clinical progression, independent of age of onset, in Niemann-Pick Disease, Type C. Am J Med Genet B Neuropsychiatr Genet 132–140 . doi: 10.1002/ajmg.b.30969.Linear

17. Thomas MSC, Annaz D, Ansari D, et al (2009) Using developmental trajectories to understand developmental disorders. J Speech Lang Hear Res 52:336–358 . doi: 10.1044/1092-4388(2009/07-0144)

18. Burnham K., Anderson D. (2002) Model selection and multimodel inference: A practical information-theoretic approach, 2nd ed. Springer, New York

19. Pinheiro JC, Bates DM (2000) Mixed-effects models in S and S-PLUS. Springer, New York

20. Diggle P (2013) Analysis of longitudinal data, Second Edition. Oxford University Press, Oxford

21. Luna B, Velanova K, Geier CF (2008) Development of eye-movement control. Brain Cogn 68:293–308 . doi: 10.1016/j.bandc.2008.08.019

22. Fioravanti F, Inchingolo P, Pensiero S, Spanio M (1995) Saccadic eye-movement conjugation in children. Vision Res 35:3217–3228 . doi: 10.1016/0042-6989(95)00152-5

23. Rottach KG, Von Maydell RD, Das VE, et al (1997) Evidence for independent feedback control of horizontal and vertical saccades from Niemann-Pick type C disease. Vision Res 37:3627–3638 . doi: 10.1016/S0042-6989(96)00066-1

24. Crespi J, Bråthen G, Quist-Paulsen P, et al (2016) Facial dystonia with facial grimacing and vertical gaze palsy with “round the houses” sign in a 29-year-old woman. Neuro-Ophthalmol 40:31–34 . doi: 10.3109/01658107.2015.1105824

25. Optican LM, Pretegiani E (2017) What stops a saccade? Philos Trans R Soc B Biol Sci 372:20160194 . doi: 10.1098/rstb.2016.0194

26. Evans WRH, Hendriksz CJ (2017) Niemann-Pick type C disease - the tip of the iceberg? A review of neuropsychiatric presentation, diagnosis and treatment. Psychiatr Bull 41:109–114 . doi: 10.1192/pb.bp.116.054072

27. Wassif CA, Cross JL, Iben J, et al (2016) High incidence of unrecognized visceral/neurological late-onset Niemann-Pick disease, type C1, predicted by analysis of massively parallel sequencing data sets. Genet Med 18:41–48 . doi: 10.1038/gim.2015.25

28. Hendriksz CJ, Anheim M, Bauer P, et al (2017) The hidden Niemann-Pick type C patient: Clinical niches for a rare inherited metabolic disease. Curr Med Res Opin 33:877–890 . doi: 10.1080/03007995.2017.1294054

Table 1. NP-C patient demographics and neurological scores.

Patient Number	Gender	Age (Years)	Disease Specific Treatment	Age at presentation of neurological features (Years)	Disability score (0-61)
NP-C 01	F	2	-	-	0
NP-C 02	M	4	-	-	0
NP-C 03	M	8	Miglustat	7	12
NP-C 04	M	8.5	-	-	0
NP-C 05	F	9	Miglustat	2	18

M=male ; F=female

Table 2. z_{pi} values for individual patients compared to the control population. L/R = left/right movements. D/U = downward/upward movements. -1.66 = 90% cutoff for normal range; -1.96 = 95% cutoff for normal range; -2.37 = 99% cutoff for normal range. $z_{pi} < -1.5$ are shown.

Patient Number	Age (Years)	Neuro Involvement	Horizontal movements				Vertical movements					
			Saccade Onset		Saccade Velocity		Saccade Onset		Saccade Velocity		Saccade Curvature	
			L	R	L	R	D	U	D	U	D	U
NP-C 01	2	No	-2.17	-	-	-	-	-	-	-	-	-
NP-C 02	4	No	-	-	-	-	-	-	-	-	-	-3.19
NP-C 04	8.5	No	-	-	-	-	-	-	-2.37	-	-2.28	-3.26
NP-C 03	8	Yes	-	-	-	-2.16	-2.17	-	-3.1	-2.83	-26.74	-16.37
NP-C 05	9	Yes	-	-	-1.53	-	-	-2.16	-4.11	-3.36	-5.65	-2.6

Figure 1. Developmental trajectory of saccade onset latency to targets in horizontal and vertical positions (msec; *neurological patients*=filled symbols; *pre-neurological patients* = open symbols; *controls*=open circles). The solid line represents the mean onset based on a quadratic fit. Dashed lines represent the boundaries of a 95% prediction interval.

Figure 2. Saccade peak velocity (measured in degrees of visual angle/sec). A) Developmental trajectory of velocity residuals after amplitude has been factored out. Left and right saccades, like upward saccades, did not change with age and have not been included. Open circles are controls, black circles are pre-neurological patients and grey triangles are neurological patients. B) Saccade velocity and amplitude plotted together. Filled symbols are neurological patients, open symbols are pre-neurological patients, and error bars represent 95% prediction intervals for controls.

Figure 3. Saccade curvature to left/right/up/down targets (light grey = 95% prediction interval for NP-C trajectories; dark grey = 95% prediction interval for control trajectories; lines = individual saccade traces).

Figure 4. Developmental trajectories for the standard deviation of saccade curvature (in degrees of visual angle. Filled symbols are neurological patients, open symbols are pre-neurological patients and open circles are controls). The solid line is the control mean based on a linear fit. Dashed lines are boundaries of the 95% prediction interval.

Appendix A. Table of patient clinical severity scores based on the Yanjanin clinical scale (2010).

Domain	Function (scale)	NP-C 01	NP-C 02	NP-C 03	NP-C 04	NP-C 05
Major	Eye-movements (0-5)	0	0	1	0	2
	Ambulation (0-5)	0	0	1	0	1
	Speech (0-5)	0	0	0	0	1
	Swallowing (0-5)	0	0	1	0	2
	Fine Motor Skills (0-5)	0	0	2	0	4
	Cognition (0-5)	0	0	3	0	3
	Hearing (0-5)	0	0	1	0	2
	Memory (0-5)	0	0	0	0	1
	Seizure (0-5)	0	0	0	0	0
Minor	Gelastic cateplexy (0-2)	0	0	0	0	0
	Narcolepsy (0-2)	0	0	1	0	1
	Behaviour (0-2)	0	0	1	0	0
	Psychiatric (0-2)	0	0	0	0	0
	Hyperreflexia (0-2)	0	0	1	0	1
	Incontinence (0-2)	0	0	0	0	0
	Auditory Brainstem Response (0-2)	0	0	0	0	0
	Respiratory (0-2)	0	0	0	0	0

Appendix B. Model results for control participants.

Model	ΔAIC	Akaike weight
Saccade onset		
Condition X Age^2	0.00	0.999
Condition + Age^2	13.83	0.001
Age^2	24.52	0.000
Condition	71.09	0.000
Intercept only	81.71	0.000
Peak velocity after amplitude is factored out		
Condition X Age	0.00	0.978
Condition + Age	8.59	0.013
Condition	9.51	0.008
Age	290.00	0.000
Saccade curvature		
Condition X Age	0.00	0.918
Condition + Age	4.85	0.081
Condition	20.13	0.000
Age	53.05	0.000

Appendix C. Models comparing pre-neurological NPC patients and controls.

Model	ΔAIC	Akaike weight
Saccade onset		
Condition X Age^2	0.00	0.519
Condition X Age^2 + Group	1.38	0.260
Condition X Age^2 + Group X Age^2	3.25	0.102
Condition X Age^2 + Group X Condition	4.07	0.068
Condition X Age^2 + Group X Condition + Group X Ag	5.80	0.029
Condition X Age^2 X Group	6.34	0.022
Peak velocity after amplitude is factored out		
Condition X Group + Condition X Age + Group X Age	0.00	0.414
Condition X Group X Age	1.00	0.251
Condition X Group + Condition X Age	1.23	0.223
Condition X Age + Group X Age	3.77	0.063
Condition X Age + Group	4.80	0.038
Group X Age + Condition	9.43	0.004
Saccade curvature		
Condition X Age X Group	0.00	0.477
Condition X Age + Condition X Group	1.68	0.206
Condition X Age + Condition X Group + Age X Group	1.73	0.201
Condition X Age + Group	4.93	0.040
Condition X Age + Age X Group	5.04	0.038
Condition X Age	5.09	0.037

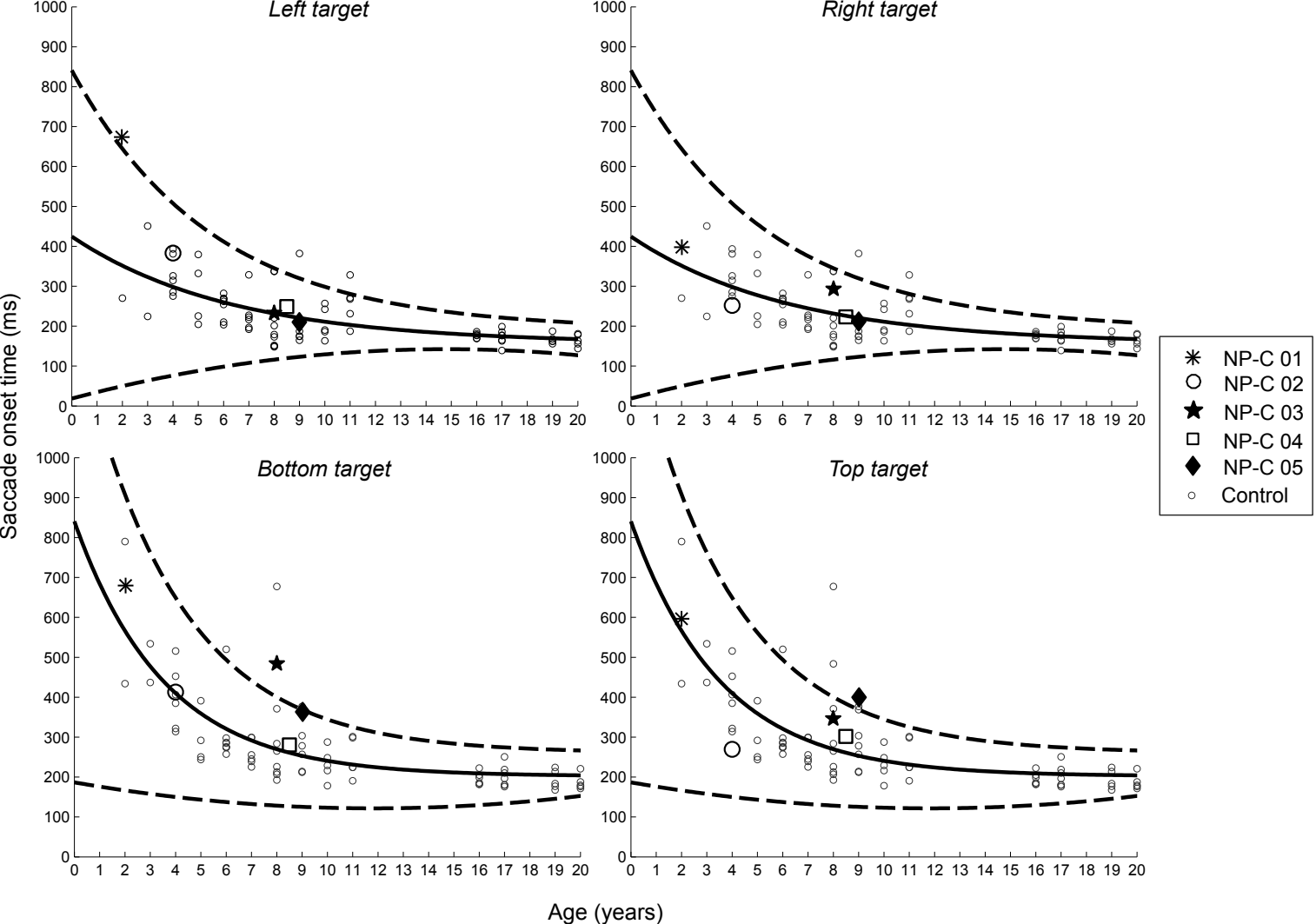
Left target
Right target
Bottom target
Top target
Saccade onset time (ms)
Age (years)
NP-C 01
NP-C 02
NP-C 03
NP-C 04
NP-C 05
Control

A

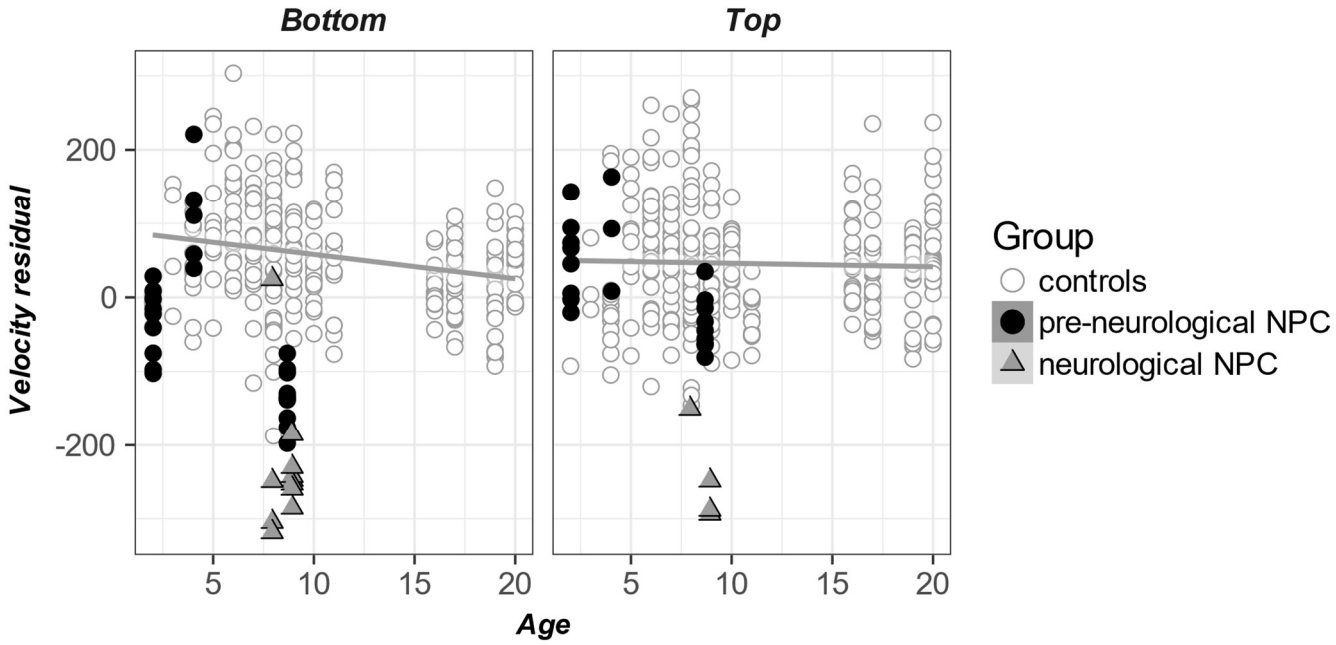
Bottom
Top
Velocity residual
200
0
-200
5
10
15
20
Age
Group
controls
pre-neurological NPC
neurological NPC

B

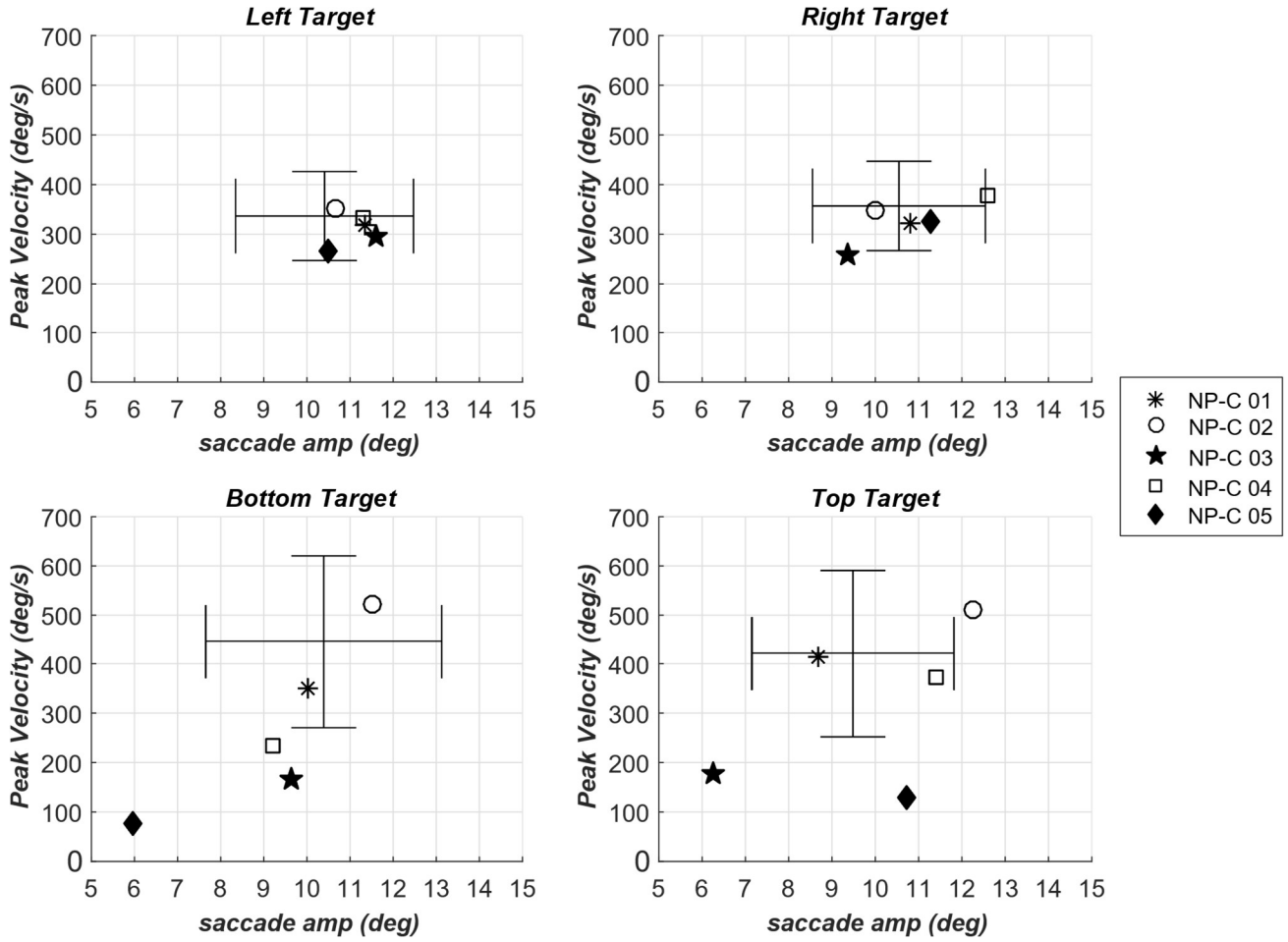
Left Target
Right Target
Bottom Target
Top Target
Peak Velocity (deg/s)
saccade amp (deg)
NP-C 01
NP-C 02
NP-C 03
NP-C 04
NP-C 05

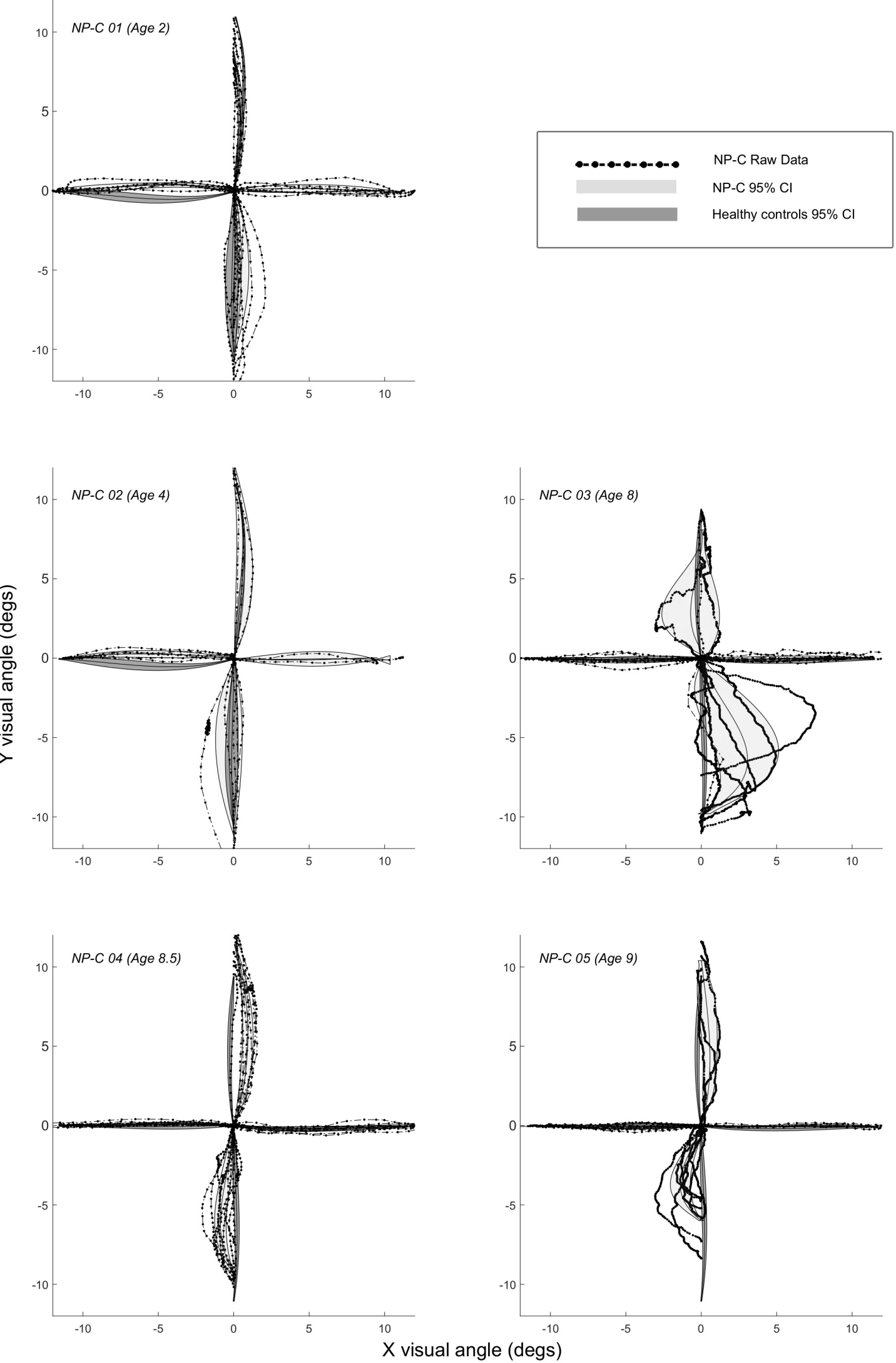
NP-C 01 (Age 2)
NP-C 02 (Age 4)
NP-C 03 (Age 8)
NP-C 04 (Age 8.5)
NP-C 05 (Age 9)
NP-C Raw Data
NP-C 95% CI
Healthy controls 95% CI
Y visual angle (degs)
X visual angle (degs)

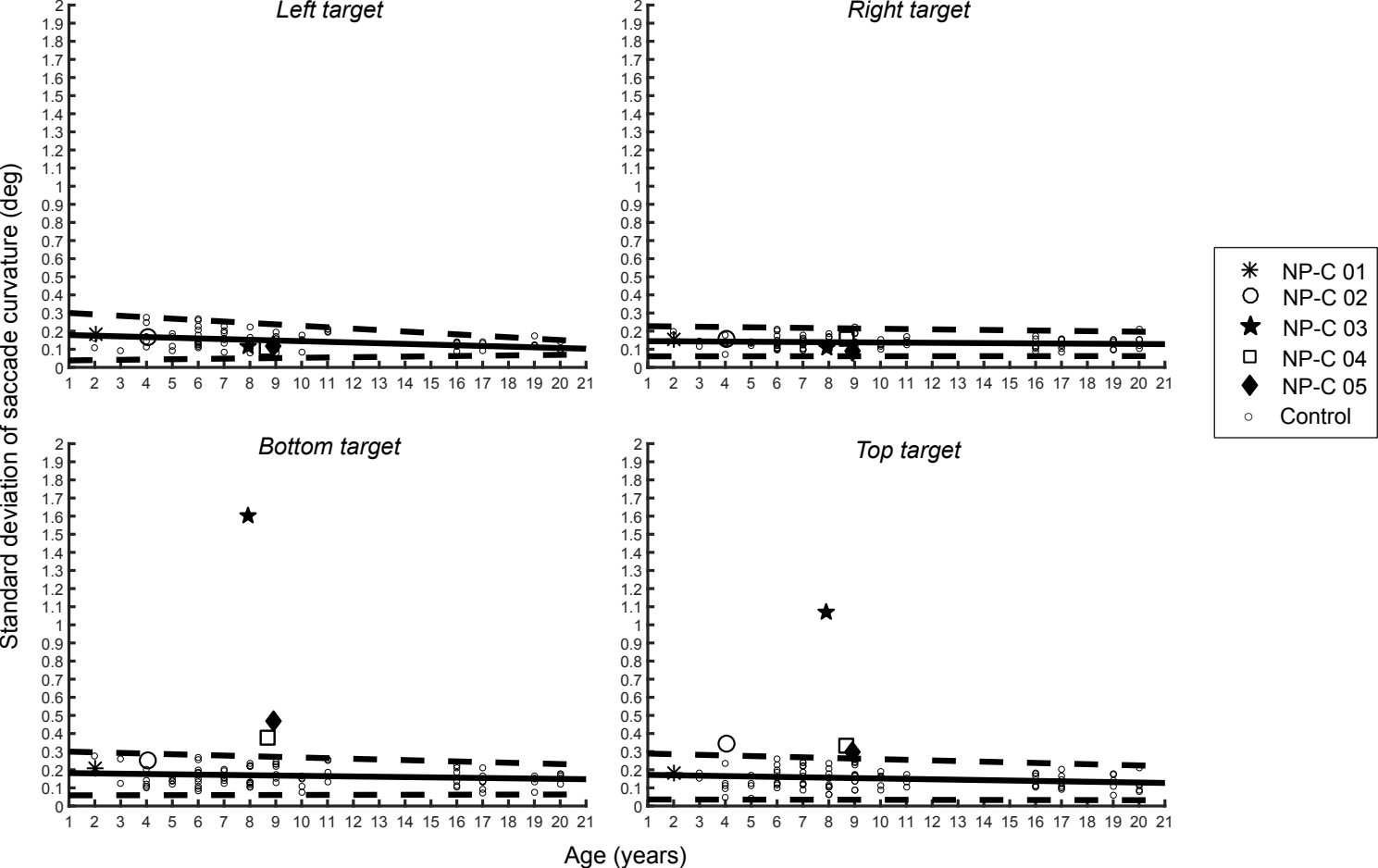
Left target
Right target
Bottom target
Top target
Standard deviation of saccade curvature (deg)
Age (years)
NP-C 01
NP-C 02
NP-C 03
NP-C 04
NP-C 05
Control